Production of wax esters in plant seed oils by oleosomal cotargeting of biosynthetic enzymes[S]

Mareike Heilmann,* **Tim Iven,*** **Katharina Ahmann,*** **Ellen Hornung,*** **Sten Stymne,[†]** **and Ivo Feussner[1],***

Department of Plant Biochemistry,* Albrecht-von-Haller-Institute for Plant Sciences, Georg-August-University, D-37077 Göttingen, Germany; and Department of Plant Breeding and Biotechnology,[†] Swedish University of Agricultural Sciences, S-23053 Alnarp, Sweden

Abstract Wax esters are neutral lipids exhibiting desirable properties for lubrication. Natural sources have traditionally been whales. Additionally some plants produce wax esters in their seed oil. Currently there is no biological source available for long chain length monounsaturated wax esters that are most suited for industrial applications. This study aimed to identify enzymatic requirements enabling their production in oilseed plants. Wax esters are generated by the action of fatty acyl-CoA reductase (FAR), generating fatty alcohols and wax synthases (WS) that esterify fatty alcohols and acyl-CoAs to wax esters. Based on their substrate preference, a FAR and a WS from *Mus musculus* were selected for this study (*Mm*FAR1 and *Mm*WS). *Mm*WS resides in the endoplasmic reticulum (ER), whereas *Mm*FAR1 associates with peroxisomes. The elimination of a targeting signal and the fusion to an oil body protein yielded variants of *Mm*FAR1 and *Mm*WS that were cotargeted and enabled wax ester production when coexpressed in yeast or *Arabidopsis*. In the *fae1 fad2* double mutant, rich in oleate, the cotargeted variants of *Mm*FAR1 and *Mm*WS enabled formation of wax esters containing >65% oleyl-oleate.[JLR] The data suggest that cotargeting of unusual biosynthetic enzymes can result in functional interplay of heterologous partners in transgenic plants.—Heilmann, M., T. Iven, K. Ahmann, E. Hornung, S. Stymne, and I. Feussner. **Production of wax esters in plant seed oils by oleosomal cotargeting of biosynthetic enzymes.** *J. Lipid Res.* 2012. **53:** 2153–2161.

Supplementary key words fatty acyl-CoA reductase • fatty alcohol • *Mus musculus* • wax ester • wax synthase

Wax esters are an important industrial commodity and serve as lubricants in numerous technical processes (1, 2). The particular feasibility of wax esters to serve as lubricants arises from their constant lubrication properties and chemical stability over a broad temperature range (2). At the molecular level, wax esters represent esters of fatty alcohols and fatty acids, and a large variety of combinations is possible, including medium, long, and very long chain lengths as well as various degrees of unsaturation of the fatty alcohol and fatty acid partners. Different molecular species of wax esters can display diverse lubrication properties. A lubricant should ideally have a low melting point and high oxidation stability. Therefore, it is desirable to have species of medium or long chain lengths having not more than one double bond in each part of the molecule. Traditionally, wax esters have been obtained from the whaling industry ("spermaceti-oil"), which relies on a dwindling natural resource and has become insignificant as a supply of wax esters for technical applications (2). The whale contains about 2,000 l of the spermaceti oil within its skull that consists mainly of oleyl-oleate. This oil was widely used as an excellent lubricant in all sorts of machinery, from fine mechanics such as watches to transmission fluids in the gear boxes in cars. Wax esters can furthermore be refined from petrochemicals. However, refining also relies on dwindling natural resources, is cost intensive, and yields wax ester mixtures of varying molecular species, which is not desirable in a technical lubricant. While some plant species, such as jojoba (*Simmondsia chinensis*), naturally produce wax esters in their oil, jojoba plants are not suitable for large-scale cultivation and produce an unfavorable blend of very long chained wax esters not suitable for technical applications (3). Thus, there is currently no large-scale biological source for wax esters. To generate wax esters, fatty acyl-CoAs must be reduced to fatty alcohols and esterified to another fatty acyl-CoA molecule. For this, only two enzymes are required, a fatty acyl-CoA

reductase (FAR) (2) and a fatty acyl-CoA:fatty alcohol acyltransferase or short wax synthase (WS). In a previous study, a combination of FAR and WS from jojoba was expressed in transgenic *Arabidopsis* seeds, and the formation of wax esters in the seed oil was observed (4). Similar to the situation in jojoba seeds, where very long chain wax esters are found (3), transgenic *Arabidopsis* seeds accumulated wax esters containing fatty alcohols of 20 carbons or longer (4). However, for technical applications, it may be desirable to use wax esters of long chain length. Therefore, it was the goal of this study to determine whether it is possible to establish wax ester production in *Arabidopsis* seeds by using enzymes from other organisms that are suitable for the production of long chain length wax esters. Two particular enzymes from mouse (*Mus musculus*) were chosen for this study, *Mm*FAR1 (5) and *Mm*WS (6), based on previously demonstrated preference of these enzymes for long chain length monounsaturated substrates. Previous characterization of *Mm*FAR1 and *Mm*WS indicated that, in the mouse, these particular enzymes serve unrelated cellular functions and in vivo localize to different organelles. For *Mm*FAR1, a role in plasmalogen biosynthesis has been proposed; the enzyme is located at the peroxisomal membrane (5). *Mm*WS might be involved in actual wax ester production not in synchronicity with *Mm*FAR1; the enzyme is located at the endoplasmic reticulum (ER) (6). Thus, despite their suitable substrate preferences, *Mm*FAR1 and *Mm*WS seem not to act together in a common pathway for wax ester production. In this study, the identification and elimination of a putative membrane-spanning domain as noncanonical peroxisomal targeting signal of *Mm*FAR1, combined with subsequent fusions of the deletion variant of *Mm*FAR1 and of full-length *Mm*WS to oleosin, a protein localized to the surface of oil bodies, resulted in enzyme variants displaying efficient interplay in heterologous expression systems. By coexpressing the so-modified variants of *Mm*FAR1 and *Mm*WS, the efficiency of wax ester production was strongly increased in yeast and *Arabidopsis* over that observed upon coexpression of the nonmodified enzymes. Moreover, the expression of the modified enzymes in an *Arabidopsis* mutant background rich in oleate ($18:1\Delta^9$) enabled an enzymatic pathway that yielded wax esters containing greater than 65% oleyl-oleate in the transgenic plants.

EXPERIMENTAL PROCEDURES

Materials

Restriction enzymes and DNA-modifying enzymes were obtained from MBI Fermentas. Standards of fatty alcohols and wax esters were obtained from Sigma, Nu-Chek-Prep, or Larodan. Methanol, chloroform, n-hexane, and iso-propanol (all HPLC grade) were from Baker. All other chemicals were from Sigma. Basic molecular biological and biochemical techniques were performed as described (7).

Cloning of *Mm*FAR, *Mm*FAR1Δc, and *Mm*WS

Codon optimized cDNAs of *Mm*FAR1 and *Mm*WS (for expression in *Brassicaceae*) were provided by Peter Denolf (Bayer Crop Science NV, Ghent, Belgium) and served as templates for all

further cloning strategies. PCR was performed to modify the cDNAs with appropriate restriction sites with following primers (restriction sites in bold): *MmFAR1-for-Eco*RI, 5′-ATGC**GAATTC**A-TGGTTTCCATCCCAGAGTACTAT-3′ / *MmFAR1-rev-Xho*I, 5′-ATG-C**CTCGAG**TTAGTATCGCATTGTGGAAGAGGC-3′ and for *MmWS*: *YFP-WS-for,* 5′-GGCATGGACGAGCTGTACAAGATGTTC-TGGCCTACTAAGAAGGAC-3′ / *MmWS-rev-Xho*I, 5′-ATGC**CTCGA-GT**TAGACGATAACCAGCTCTTGTGT-3′. Engineering of the truncated *MmFAR1Δc* construct was a result of hydropathy analysis, which revealed two putative transmembrane domains at the very C terminus of *Mm*FAR1, and this information was used to design primers excluding the C-terminal coding region: *MmFAR1Δc-for-Eco*RI (see above for *MmFAR1*) and *MmFAR1Δc-rev-Xho*I, 5′-GGAT-GC**CTCGAG**TTATCTGATGTTGCGAAGCTTGTT-3′.

Fusion constructs for particle bombardment

Plasmids carrying the authentic clones for mCherry and EYFP were provided by Martin Fulda (Georg-August-University, Göttingen, Germany). The *mCherry* cDNA was modified by using the following primers: *mCherry-for-Bam*HI, 5′-ATGCGGATCCATGGTGAGCAA-GGGCGAGGAGGAT-3′ and *mCherry-rev-Eco*RI, 5′-ATGCGAAT-TCCTTGTACAGCTCGTCCATGCCGCC-3′. The resulting amplicon was moved into the plasmid *pUC18Entry2* (8) as *Bam*HI/*Eco*RI fragment, creating the plasmid *pUC18Entry2-mCherry*. The PCR products representing *Mm*FAR1 and *Mm*FAR1Δc were moved as *Eco*RI/*Xho*I fragments into pUC18Entry2-mCherry, creating the plasmids *mCherry-MmFAR1* and *mCherry-MmFAR1Δc*, respectively. To create *Oleo3-mCherry-MmFAR1Δc* and *Oleo3-mCherry*, the *Oleosin3* cDNA was amplified from *Arabidopsis* Col-0 cDNA with the respective primers (restriction sites in bold; SL stands for short linker and is marked in italics within the primer sequence): *Oleo3-Sal*I-*for,* 5′-GGCCATGC**GTCGAC**ATGGCGGACCAAACAAGAACC-3′ / *Oleo3-Bam*HI-*rev-SL,* 5′-GGCCATGC**GGATCC**TCCTGCACCTGCA-GAAACTTGTTGGTGTTGGAC-3′. The *Oleosin3* amplicon was then moved as *Sal*I/*Bam*HI fragment into *pUC18Entry2-mCherry-MmFAR1Δc* or into *pUC18Entry2-mCherry,* resulting in the plasmids *Oleo3-mCherry-MmFAR1Δc* and *Oleo3-mCherry*. The *EYFP*-fusion constructs were generated by overlap extension PCRs, engineering hybrid genes without the use of restriction enzymes. First, *EYFP, MmWS* and *Oleosin3* were amplified individually from the respective cDNA templates using the following primers: *EYFP-for-Bam*HI 5′-ATGCGGATCCATGGTGAGCAAGGGCGAG-GAGCTG-3′ or *Oleo3-EYFP-for,* 5′-TCCAACACCAACAAGTTTCTA-TGGTGAGCAAGGGCGAGGAG-3′/*EYFP-MmWS-rev,* 5′-GTCCT-TCTTAGTAGGCCAGAACATCTTGTACAGCTCGTCCATGCC-3′; for *MmWS*: *YFP-WS-for,* (see above) / *MmWS-rev-Xho*I (see above) and for *Oleosin3*: *Oleo3-for-Kpn*I, 5′-GGCCATGC**GGTACC**ATGG-CGGACCAAACAAGAACC-3′/*Oleo3-EYFP-rev,* 5′-CTCCTCGCCC-TTGCTCACCATAGAAACTTGTTGGTGTTGGA-3′. The amplicons were fused in a subsequent PCR reaction using primers *EYFP-for-Bam*HI/*MmWs-rev-Xho*I and *Oleo3-for-Kpn*I/*MmWs-rev-Xho*I, respectively, generating the fusion gene constructs *EYFP-MmWS* and *Oleo3-EYFP-MmWS*. The fusion PCR products were moved into *pUC18Entry* as *Bam*HI/*Xho*I or as *Kpn*I/*Xho*I fragments. All constructs were transferred by Gateway technology (Invitrogen) from *pUC18Entry2* to the *pCAMBIA33.1* plasmid, an expression vector containing the cauliflower mosaic virus (CMV) 35S promoter, an *att*R1/R2 gateway cassette, and a CMV 35S terminator. The *pCAMBIA33.1* vector was modified as described (8).

Particle bombardment

Onion epidermal cells were transformed by bombardment with plasmid-coated 1 µm gold particles with a helium-driven particle accelerator (PDS-1000/He; Bio-Rad) using 1,350 psi rupture discs and a vacuum of 27 inches of mercury. Gold particles were

coated with 4–8 µg of plasmids. After bombardment, the onion epidermal cells were incubated for 14–20 h.

Microscopy and imaging

Images were recorded using an Olympus BX51 epifluorescence microscope.

Preparation of yeast expression constructs

The open reading frames of *mCherry-MmFAR1*, *mCherry-MmFAR1Δc*, and *Oleo3-mCherry-MmFAR1Δc* were moved as *Bam*HI-*Xho*I or *Sal*I-*Xho*I fragments, respectively, into the mcs2 of *pESC-URA* (Stratagene). *EYFP-MmWS* and *Oleo3-EYFP-MmWS* were amplified as fusion constructs with the following primer combinations: *EYFP-for-Spe*I, 5′-GGCCATGC**ACTAGT**ATGGTGAGCAA-GGGCGAGGAGCTGTTC-3′ or *Oleo3-for-Spe*I, 5′-GGCCATGC**AC-TAGT**ATGGCGGACCAAACAAGAACCCAT-3′ and *MmWS-rev-Sac*I, 5′-GGCCATGC**GAGCTC**TTAGACGATAACCAGCTCTTG-TGT-3′. The resulting PCR products were ligated into the mcs1 site of *pESC-URA*, yielding *pESC-URA-mCherry-MmFAR1_EYFP-MmWS*, *pESC-URA-mCherry-MmFAR1Δc_EYFP-MmWS*, *pESC-URA-Oleo3-mCherry-MmFAR1Δc_EYFP-MmWS*, and *pESC-URA-Oleo3-mCherry-MmFAR1Δc_Oleo3-EYFP-MmWS*.

Constructs for stable expression in Arabidopsis

Two different entry vectors were generated based on the pUC19 backbone. For this purpose, cDNA-stretches containing a napin promoter (9), a multiple cloning site, and an octane-synthase (OCS) terminator (10) were created by fusion-PCRs that were flanked by Gateway attachment sites. Fragments flanked by attL1 and attL4 or attR4 and attL2, respectively, were moved into pUC19 as *Hind*III/*Eco*RI fragments, yielding the plasmids pENTRY-A and pENTRY-D. The open reading frames of *mCherry-MmFAR1*, *Oleo3-mCherry-MmFAR1Δc*, *EYFP-MmWS*, and *Oleo3-EYFP-MmWS* were amplified as fusion constructs with the following primer combinations: for *mCherry-MmFAR1*, *mCherry-for-Sal*I 5′-GGATGC**GTCGAC**ATG-GTGAGCAAGGGCGAGGA-3′/*FAR1-rev-Not*I 5′-GGCCATGC**GC-GGCCGC**TTAGTATCGCATTGTGGAAG-3′; for *Oleo3-mCherry-MmFAR1Δc*, *Oleo3-for-Sal*I 5′-GGCCATGC**GTCGAC**ATGGCGGACC-AAACAAGAACC-3′/*FAR1c-rev-Not*I 5′-GGCCATGC**GCGGCCGC**T-TATCTGATGTTGCGAAGCTT-3′; for *EYFP-WS*, *YFP-for-Sal*I 5′-GGC-CATGC**GTCGAC**ATGGTGAGCAAGGGCGAGGA-3′/*WS-rev-Not*I 5′-GGCCATGC**GCGGCCGC**TTAGACGATAACCAGCTCTT-3′, and for *Oleo3-EYFP-WS*, *Oleo3-for-Sal*I 5′-GGCCATGC**GTCGAC**A-TGGCGGACCAAACAAGAACC-3′/ *WS-rev-Not*I 5′-GGCCATGC-**GCGGCCGC**TTAGACGATAACCAGCTCTT-3′. The resulting PCR products were moved as *Sal*I/*Not*I fragments into the mcs site of pENTRY-A, yielding *pENTRY-A-mCherry-MmFAR1* or *pENTRY-A-Oleo3-mCherry-MmFAR1Δc,* respectively, or into the mcs of pENTRY-D, yielding *pENTRY-D-EYFP-MmWS* or *pENTRY-D-Oleo3-EYFP-MmWS*, respectively. Construct combinations were transferred by Dual-Gateway technology (Invitrogen) from pENTRY-A and pENTRY-D into the *pCAMBIA33.0* plasmid, a plant transformation vector containing an *att*R1/R2 gateway cassette. The *pCAMBIA33.0* vector was modified as described (8). This results in the constructs *pCAMBIA33.0- pNAPIN::mCherry-MmFAR1-OCS_pNAPIN::EYFP-MmWS-OCS*, *pCAMBIA33.0-pNAPIN::Oleo3-mCherry-MmFAR1-OCS_pNAPIN::EYFP-MmWS-OCS*, and *pCAMBIA33.0- pNAPIN::Oleo3-mCherry-MmFAR1-OCS_pNAPIN::Oleo3-EYFP-MmWS-OCS*.

Arabidopsis transformation

Arabidopsis thaliana Col-0 plants were transformed by floral dipping (11). The respective transformants (T1-plants) were grown on soil and selected by ammonium glufosinate treatment. T2-seeds of the selected plants were collected from individual T1-plants and analyzed.

Yeast expression

Saccharomyces cerevisiae strain H1246 defective in storage lipid accumulation (12) was transformed with the different constructs as described (8). Expression cultures were grown for 48–96 h at 30°C in the presence of 2% (w/v) galactose. When indicated, primary alcohol (16:0-OH) was dissolved in chloroform and added to the culture medium to a final concentration of 0.1%. Cells were harvested by centrifugation at 700 g for 5 min and then used for further analysis. The host strain transformed with the empty vector (pESC-URA) was used as negative control in all experiments.

Wax ester isolation

For lipid analysis in yeast, expression was carried out with 10 ml cultures. Equal OD_{600} units of the yeast cell cultures were harvested, and fresh weight was determined. The cell pellets were homogenized by vigorous shaking (1, 000 rpm) with the help of glass beads (0.7 mm diameter) in 2 ml chloroform/methanol 1:2 (v/v). As an internal standard, 12:0/12:0 wax ester was added. The mixture was incubated for 20 min, followed by the addition of 2 ml n-hexane/diethyl ether 65:35 (v/v) and shaking for 20 min. The resulting organic phases were combined and dried under N_2. The remaining lipids were dissolved in 30 µl of chloroform. Isolation and separation of wax esters were achieved by preparative thin-layer chromatography (TLC) using appropriate standards and with n-hexane/diethyl ether/glacial acetic acid (80:20:1, v/v/v) as developing solvent. The wax esters were scraped from TLC plates and analyzed by GC-MS. Separation of fatty alcohols was achieved by TLC using n-hexane/diethyl ether/ glacial acetic acid (65:35:1, v/v/v) as developing solvent modified from the method described previously (6).

For extraction of *Arabidopsis* seed oil, 5 mg seeds were homogenized after addition of 2 ml chloroform/methanol 1:1 (v/v) and 9.8 nmol 17:0/17:0 wax ester as internal standard by using a Potter-Elvejhem device (Heidolph) equipped with a PFTE pestle. The homogenate was transferred to an 8 ml Teflon-lined screw-cap glass tube. Lipids were extracted for 20 min and then for another 20 min with 2 ml n-hexane/diethyl ether 65:35 (v/v). Nonsoluble cell debris was pelleted by 5 min centrifugation at 450 g. The resulting organic phases were combined and dried under streaming N_2. The remaining lipids were dissolved in 30 µl of chloroform. Isolation and separation of wax esters was achieved by preparative TLC using silica gel 60 glass plates 0.25 mm × 20 cm × 20 cm (Merck) with n-hexane/diethyl ether/glacial acetic acid (80:20:1, v/v/v) as developing solvent. The wax esters were scraped from TLC plates and recovered from the silica by extracting twice with 1 ml hexane. The solvent was evaporated under streaming N_2. For ESI-MS/MS measurement, the wax esters were dissolved in 200 µl chloroform/methanol 1:2 (v/v) containing 5 mM ammonium acetate.

GC-MS analysis

For GC-MS quantification of total wax ester load of yeast extracts, wax ester preparations were dissolved in 20 µl chloroform, and 2 µl were subjected to GC-MS analysis using a Polaris Q mass selective detector connected to a Trace gas chromatograph (Thermo Finnigan) equipped with a capillary column (Rxi-5ms, 15 m × 0.25 mm, 0.25 µm film thickness; Restek). Helium was used as carrier gas (1.5 ml min^{-1}). The temperature gradient was 2 min 60°C, 60–200°C at 40°C min^{-1}, 2 min at 200°C, 200–340°C at 3°C min^{-1}, and 340°C for 16 min. The wax esters were detected by electron impact ionization (-70 eV, ion source 200°C, Aux-line 340°C) in a mass range of 50–730 amu. The wax esters were quantified by comparison of the peak area of the 12:0/12:0 internal standard signal to peak areas of the analyte wax esters using Xcalibur quality browser V1.4 (Thermo Scientific).

ESI-MS/MS analysis

The analysis of wax esters from *Arabidopsis* seed oil was performed using an Applied Biosystems 3200 hybrid triple quadrupole/linear ion trap mass spectrometer (ABSciex). Direct injection nanoelectrospray ionization analysis (nanoESI) was achieved using a chip ion source (TriVersa NanoMate; Advion BioSciences). Ten microliters of wax ester extract was subjected to ESI in positive ionization mode with ionization voltage of 1.7 kV and backpressure of 0.2 psi. The mass analyzers were adjusted to a resolution of 0.7 amu full width at half-height. The ion source temperature was $40°C$, and the curtain gas was set at 10 (given in arbitrary units). Intensity profiles of 401 wax esters covering acyl chain combinations at the acyl-COOH or acyl-OH moiety with carbon numbers (C) of 16, 18, 20, 22, and 24, and saturation levels from 0 to 3 double bonds (DB) were monitored by applying multiple reaction monitoring mode (MRM) with optimized MS parameters for predefined wax ester prototype groups. As MRM precursor ion, the Q1 mass analyzer selected for the ammonium adduct of the wax esters $[M+NH_4]^+$, and the Q3 mass analyzer selected for the $[RCO_2H_2]^+$ or the $[RCO^+]^+$ fragment ion (R represents the fatty acid moiety). For quantification, calibration curves of representative wax ester standards of each prototype group were prepared applying the following MS parameters (supplementary Fig. II and supplementary Tables I and II): [Group 1] for saturated wax esters with C32–36 declustering potential (DP) 65 V, entrance potential (EP) 4.5 V, collision energy (CE) 25 V, and MRM transition of $[M+NH_4]^+/[RCO_2H_2]^+$; [Group 2] for wax esters with C32–36 and one DB in the acyl-COOH moiety DP 65 V, EP 4.5 V, CE 25 V, and MRM transition of $[M+NH_4]^+/[RCO_2H_2]^+$; [Group 3] for wax esters with C32–36 and one DB in the acyl-OH moiety DP 65 V, EP 4.5 V, CE 25 V, and MRM transition of $[M+NH_4]^+/[RCO_2H_2]^+$; [Group 4] for wax esters with C32–36 and 2–3 DB in the acyl-COOH moiety DP 60 V, EP 4.5 V, CE 25 V, and MRM transition of $[M+NH_4]^+/[RCO^+]^+$; [Group 5] for wax esters with C32–36 and 2–6 DB DP 60 V, EP 4.5 V, CE 25 V, and MRM transition of $[M+NH_4]^+/[RCO^+]^+$; [Group 6] for saturated wax esters with C38–48 DP 57 V, EP 4.5 V, CE 27 V, and MRM transition of $[M+NH_4]^+/[RCO_2H_2]^+$; [Group 7] for wax esters with C38–48 and one DB in the acyl-COOH moiety DP 65 V, EP 4.5 V, CE 24 V and MRM transition of $[M+NH_4]^+/[RCO_2H_2]^+$; [Group 8] for wax esters with C38-48 and one DB in the acyl-OH moiety DP 65 V, EP 4.5 V, CE 24 V, and MRM transition of $[M+NH_4]^+/[RCO_2H_2]^+$; [Group 9] for wax esters with C32–36 and 2–6 DB DP 60 V, EP 4.5 V, CE 25 V, and MRM transition of $[M+NH_4]^+/[RCO^+]^+$. Quantification was carried out using a calibration curve of intensity (m/z) ratios of [prototype WE]/[17:0/17:0 WE] versus molar amounts of prototype WE (20–20,000 pmol). To correct for false positive signals that occur due to unspecific detection of sterol esters or unspecific signal background caused by the matrix, we performed a background correction by subtraction of the mean molar amounts of each MRM transition that were detected in six individual empty vector control lines from the molar amounts detected in the transgenic lines (supplementary Table II).

RESULTS

Elimination of a noncanonical C-terminal targeting signal from *Mm*FAR1 results in cytosolic localization of the truncated variant, *Mm*FAR1Δc, in onion epidermal cells

*Mm*FAR1 has previously been reported to localize to peroxisomes in mouse (5). To test whether this localization pattern would also hold true for plant cells, *Mm*FAR1 was transiently expressed in onion epidermal cells as a fusion to mCherry, and the fluorescence distribution was monitored (**Fig. 1A**). The mCherry fluorescence decorated punctate structures that colocalized with EYFP-tagged peroxisomal malate dehydrogenase (pMDH:EYFP), a peroxisomal marker protein (13) (Fig. 1A), thus confirming peroxisomal localization of mCherry:*Mm*FAR1 in onion cells. The amino acid sequence of *Mm*FAR1 does not contain a recognizable plant peroxisomal targeting signal (PTS) (14, 15). To rationalize peroxisomal targeting of *Mm*FAR1, we hypothesized that a C-terminal region of 66 amino acids (Fig. 1B), which may represent a transmembrane domain according to TMHMM prediction (16), may anchor *Mm*FAR1 to the peroxisomal membrane. This notion was based on previous reports that peroxins, components of the peroxisomal import machinery, require a transmembrane region for transport to and association with peroxisomes (17). To release *Mm*FAR1 from the peroxisome, a deletion construct lacking the C-terminal 66 amino acids, *Mm*FAR1Δc, was generated. When mCherry-tagged *Mm*FAR1Δc was expressed in onion epidermal cells, peroxisomal localization was lost and the enzyme localized to the cytosol (Fig. 1C).

Fusion of *Mm*FAR1Δc and *Mm*WS to oleosin tags cotargets the enzymes to oleosin-accumulating structures of onion epidermal cells

To achieve efficient interplay of *Mm*FAR1Δc and *Mm*WS at a cellular location capable of accommodating storage lipids, it was attempted to cotarget the enzymes to oil bodies. Therefore, mCherry:*Mm*FAR1Δc was fused to *Arabidopsis* oleosin3 (Oleo3), a known component of oil body envelopes in *Arabidopsis* (18). When transiently expressed in onion epidermal cells, the fluorescence-tagged fusion protein Oleo3:mCherry:*Mm*FAR1Δc decorated punctate structures that were different from pMDH:EYFP-labeled peroxisomes (**Fig. 2A**) and coincided with Oleo3-labeled structures (Fig. 2B). In addition, Oleo3:mCherry:*Mm*FAR1Δc displayed limited partial overlap with EYFP:*Mm*WS (Fig. 2C). When EYFP:*Mm*WS was also fused to Oleo3, the resulting fusion protein Oleo3:EYFP:*Mm*WS decorated punctate structures that coincided with those decorated by Oleo3:mCherry: *Mm*FAR1Δc (Fig. 2D), indicating successful cotargeting of both enzymes to Oleo3-labeled structures.

Cotargeting of the biosynthetic pathway enhances wax ester biosynthesis in yeast and Arabidopsis

To test whether cotargeting of *Mm*FAR1 and *Mm*WS had beneficial effects on wax ester production upon heterologous expression, the accumulation of reaction products was monitored in yeast upon expression of the original enzymes as well as their modified variants. First, it was tested whether the modified variants of *Mm*FAR1 were capable of generating fatty alcohols, which are not naturally present in yeast. When mCherry:*Mm*FAR1, mCherry:*Mm*FAR1Δc, or Oleo3:mCherry:*Mm*FAR1Δc were expressed in yeast, formation of fatty alcohols was observed in all cases (**Fig. 3A**, FA-1-OH). Importantly, the modified variants of *Mm*FAR1 were not impaired in producing fatty alcohols, as equivalent amounts of such were formed upon expression
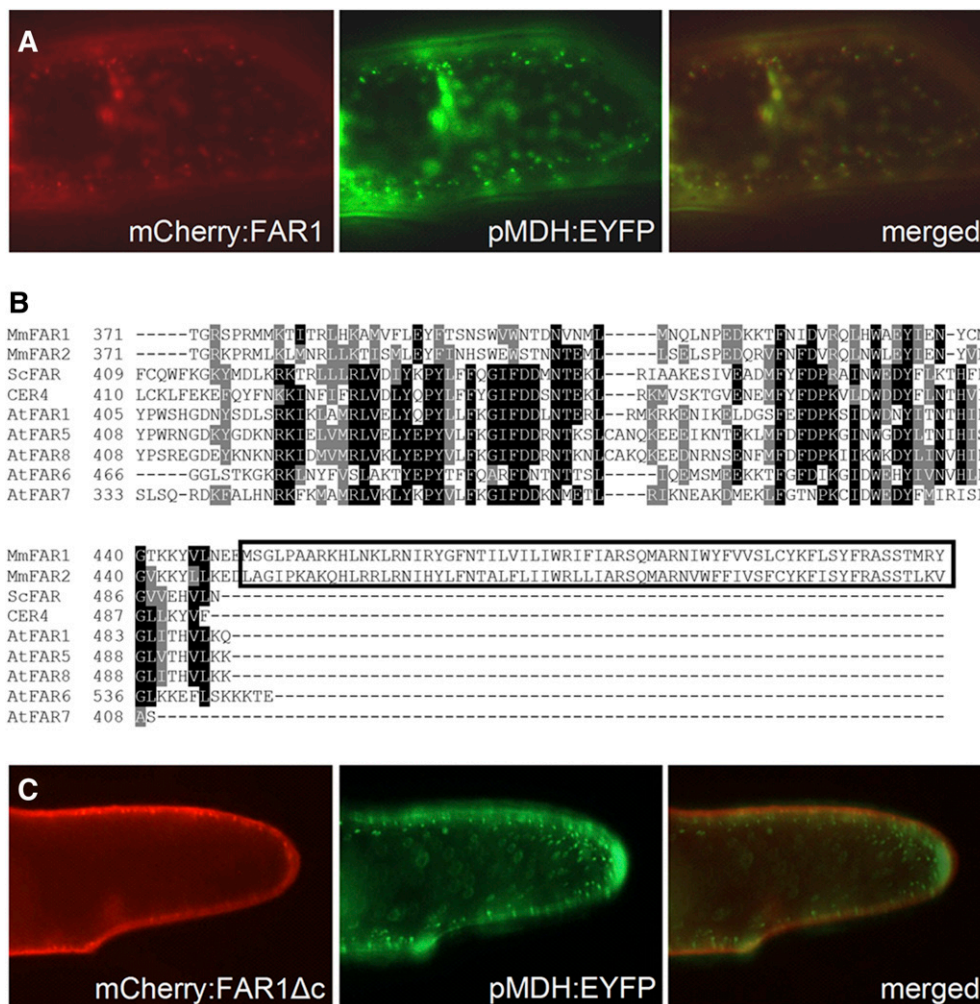
Fig. 1. Localization of mCherry-tagged *Mm*FAR1 in onion epidermal cells. (A) Coexpression of mCherry:*Mm*FAR1 and the peroxisomal marker pMDH:EYFP, as indicated. Right panel, merged image. (B) Alignment of deduced amino acid sequences of FARs from various biological sources. The C-terminal extension of *Mm*FAR1 and *Mm*FAR2 is highlighted. The highlighted sequence was deleted in *Mm*FAR1Δc. (C) Coexpression of mCherry:*Mm*FAR1Δc and pMDH:EYFP, as indicated. Right panel, merged image. Images are representative for results from five independent transformation experiments, each yielding >50 transformed cells. Mm, *Mus musculus*; CER4, Arabidopsis *Eceriferum Mutant* 4; Sc, *Saccharomyces cerevisiae*; At, *Arabidopsis thaliana*.

of mCherry:*Mm*FAR1, mCherry:*Mm*FAR1Δc, or Oleo3:mCherry:*Mm*FAR1Δc. After the production of fatty alcohols in yeast was successful, variants of *Mm*WS were additionally expressed to test for wax ester production (Fig. 3B). Wax esters are not naturally produced by yeast. When nonmodified *Mm*FAR1 and *Mm*WS were coexpressed in yeast, wax esters were successfully produced (Fig. 3B). Successive fusion of mCherry:*Mm*FAR1Δc and EYFP:*Mm*WS to Oleo3-tags resulted in increased production of wax esters, and maximum amounts were detected in yeast coexpressing Oleo3:mCherry:*Mm*FAR1Δc and Oleo3:EYFP:*Mm*WS (Fig. 3B). The wax esters accumulating in yeast expressing the original or modified variants of mCherry:*Mm*FAR and EYFP:*Mm*WS were quantified, as indicated and shown in Fig. 3C. Based on the quantitative analysis, the combined expression of Oleo3-fusions of *Mm*FAR1Δc and *Mm*WS resulted in a wax ester yield that was increased by approximately 100% (Fig. 3C). Upon successful establishment of

a cotargeted pathway for wax ester biosynthesis in yeast, equivalent constructs were tested in transgenic *Arabidopsis* plants (**Fig. 4**). Wax esters are not naturally produced by *Arabidopsis* in the seed oil (4). Similar to the situation in yeast, seed-specific expression of nonmodified mCherry:*Mm*FAR1 and EYFP:*Mm*WS resulted in the formation of a modest amount of wax esters in seeds (Fig. 4A). The seed-specific expression of Oleo3-fused mCherry:*Mm*FAR1Δc and EYFP:*Mm*WS in *Arabidopsis* resulted in increased levels of wax esters, and maximum amounts of wax esters were detected in *Arabidopsis* seeds coexpressing Oleo3:mCherry:*Mm*FAR1Δc and Oleo3:EYFP:*Mm*WS (Fig. 4A).

Designer wax esters produced from tailored substrate pools

After wax ester production had been established with the mouse enzymes in transgenic *Arabidopsis* seeds, experiments were conducted to determine the molecular
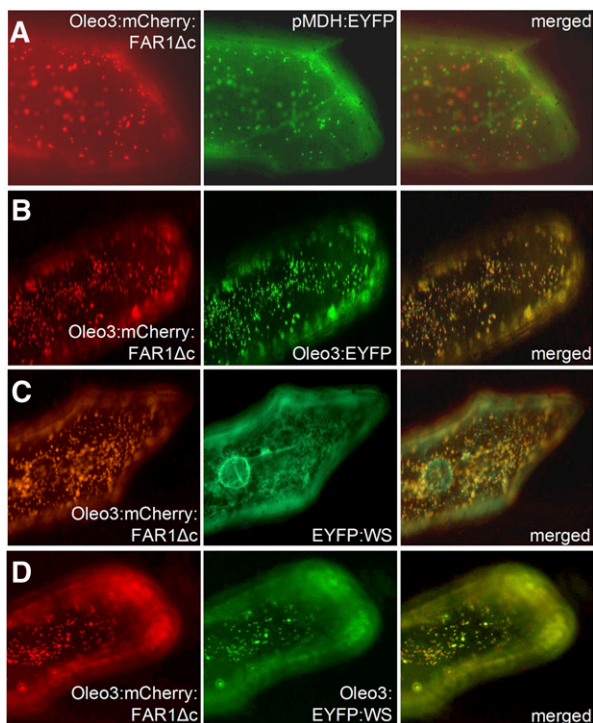
Fig. 2. Colocalization of retargeted fusion proteins Oleo3-mCherry-*Mm*FAR1Δc and Oleo3-EYFP-*Mm*WS on oleosomes of onion epidermis cells. (A) Subcellular localization of Oleo3:mCherry:FAR1Δc in vivo compared with a coexpressed pMDH:EYFP marker. (B) Localization of Oleo3:mCherry:FAR1Δc compared with Oleo3:EYFP. (C) Localization of Oleo3:mCherry:FAR1Δc compared with *Mm*WS:EYFP. (D) Localization of Oleo3:mCherry:*Mm*FAR1Δc compared with Oleo3:EYFP:*Mm*WS. Right panels, merged images. Images are representative for results from five independent transformation experiments, each yielding >50 transformed cells.

composition of the wax esters produced. The analysis of molecular wax ester species formed in transgenic *Arabidopsis* seeds showed that up to 399 wax ester species were formed upon expression of variants of mCherry:*Mm*FAR1 and EYFP:*Mm*WS, but only about 10 species accumulated to a relative abundance of more than 2%. The highest 10 representative species are shown in **Fig. 5A–C**. mCherry:*Mm*FAR1 and EYFP:*Mm*WS had been selected for pathway engineering based on their preference for monounsaturated substrates with long chain length (5, 6). However, the predominant wax ester species detected in wild-type *Arabidopsis* background were gondoyl-linoleate ($20:1^{\Delta11Z}/18:2$), oleyl-linoleate (18:1/18:2), arachidyl-linoleate (20:0/18:2), and gondoyl-linolenate ($20:1^{\Delta11Z}/18:3$), likely reflecting the combined effects of abundant linoleate substrate and effective conversion by the mouse enzymes. Although the composition of molecular wax ester species detected varied somewhat among transgenic plants expressing mCherry:*Mm*FAR1/EYFP:*Mm*WS, Oleo3:mCherry:*Mm*FAR1Δc/EYFP:*Mm*WS, or Oleo3:mCherry:*Mm*FAR1Δc/Oleo3:EYFP:*Mm*WS (Fig. 5A–C), it is clear that the presence of multiple routes of fatty acid conversion in wild-type *Arabidopsis* seeds prevented the accumulation of a defined and desired molecular species. To facilitate the desired production of oleyl-oleate wax
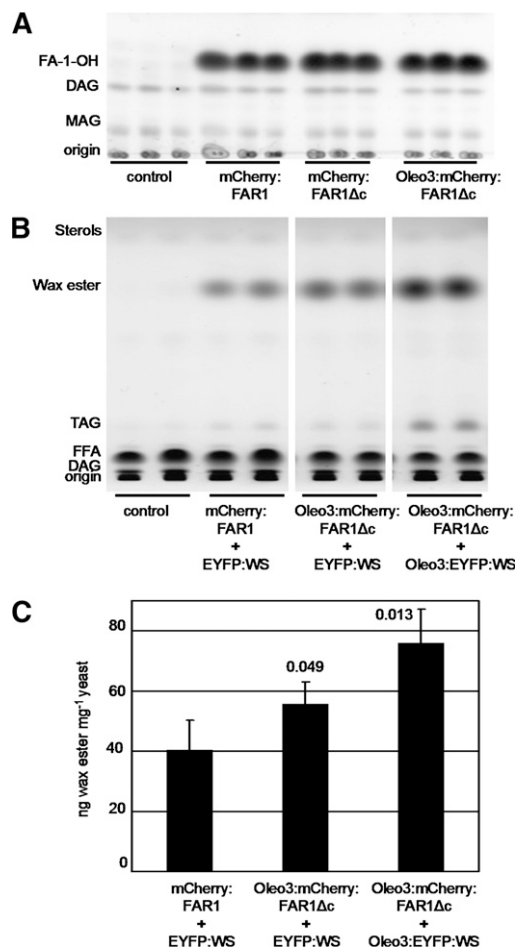

Fig. 3. Accumulation of reaction products of *Mm*FAR1 and *Mm*WS variants in transgenic yeast. (A) Unmodified mCherry:*Mm*FAR1, mCherry:*Mm*FAR1Δc, or Oleo3:mCherry:*Mm*FAR1Δc were expressed in yeast, and the production of fatty alcohols was monitored by thin-layer chromatography. Yeast transformed with an empty vector was used as a control, as indicated. (B) Different fusion variants of *Mm*FAR1 and *Mm*WS were coexpressed in yeast to test for the production of wax esters arising from the functional interplay of the two enzymes, as indicated. Expressed proteins were encoded on a single vector; yeast transformed with an empty vector was used as a control, as indicated. (C) Quantification of wax esters produced by different combinations of *Mm*FAR and *Mm*WS based on GC/MS-analysis of wax esters reisolated from thin-layer chromatography plates as shown in (B). Data in (A) and (B) are representative for five independent experiments yielding similar results. Data in (C) represent mean ± SD from three independent experiments. The values above the bars represent the *P*-values of Student *t*-test between mCherry:*Mm*FAR1 + EYFP:*Mm*WS and Oleo3:mCherry:*Mm*FAR1Δc + EYFP:*Mm*WS, as well as mCherry:*Mm*FAR1 + EYFP:*Mm*WS and Oleo3:mCherry:*Mm*FAR1Δc + Oleo3:EYFP:*Mm*WS transgenic lines. DAG, diacylglycerol; FA-1-OH, fatty acid primary alcohol; FFA, free fatty acid; MAG, monoacylglycerol.

esters, wax ester formation by Oleo3:mCherry:*Mm*FAR1Δc and Oleo3:EYFP:*Mm*WS was monitored in the *Arabidopsis fae1 fad2* double mutant rich in oleate (19). The *fae1 fad2* double mutant is deficient in ER-resident elongation of fatty acids beyond 18 carbons by FAE1 (20) and lacks the ER-resident fatty acid desaturase FAD2 required for the production of polyunsaturated fatty acids, such as linoleic and linolenic acids (21), resulting in
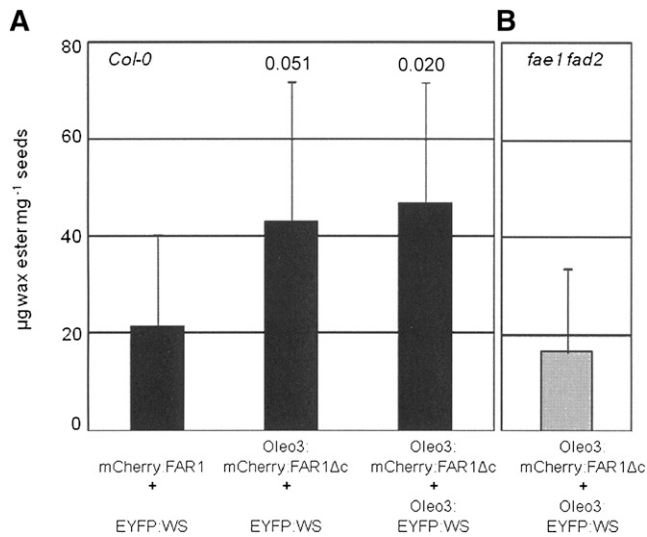
Fig. 4. Total wax ester accumulation determined by direct infusion nano-ESI-MS^2 analysis in seeds of *Arabidopsis*. (A) Col-0 wt and (B) Col-0 *fae1 fad2* mutant background expressing the indicated transgene combinations. Shown is the mean wax ester accumulation (+ SD) of seed pools of individual heterozygous T2 lines with (A) 10 lines for mCherry:*Mm*FAR1 + EYFP:*Mm*WS, 14 lines for Oleo3:mCherry:*Mm*FAR1Δc + EYFP:*Mm*WS, 10 lines for Oleo3:mCherry:*Mm*FAR1Δc + Oleo3:EYFP:*Mm*WS, and (B) 6 lines for Oleo3:mCherry:*Mm*FAR1Δc + Oleo3:EYFP:*Mm*WS analyzed. The values above the bars represent the *P*-values of Student *t*-test between mCherry:*Mm*FAR1 + EYFP:*Mm*WS and Oleo3:mCherry:*Mm*FAR1Δc + EYFP:*Mm*WS, as well as mCherry:*Mm*FAR1 + EYFP:*Mm*WS and Oleo3:mCherry:*Mm*FAR1Δc + Oleo3:EYFP:*Mm*WS transgenic lines.

the accumulation of about 85% oleate in the seed (19). When Oleo3:*Mm*FAR1Δc and Oleo3:EYFP:*Mm*WS were expressed in the *fae1 fad2* mutant background, wax esters were produced (Fig. 4B). Although the overall yield of wax esters was lower than that observed upon expression of Oleo3:mCherry:*Mm*FAR1Δc and Ole3:EYFP:*Mm*WS in wild-type *Arabidopsis* (Fig. 4A), the quality of the wax esters was substantially changed from that observed with any of the constructs used in the wild-type background (Fig. 5).
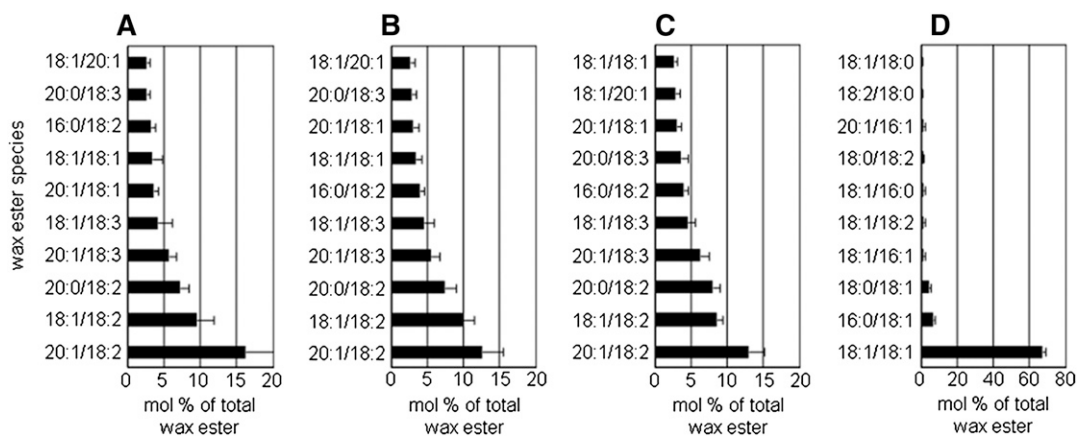
Importantly, the desired oleyl-oleate wax esters accounted now for greater than 65% of wax esters produced in the *fae1 fad2* background (Fig. 5D), whereas in wild-type, no single wax ester species exceeded 16%, regardless of what expression constructs were used (Fig. 5A–C). Further analysis of fatty alcohols and fatty acids found in wax esters formed in wild-type seeds or the *fae1 fad2* mutant indicates that oleyl-alcohol levels were higher than oleate levels in all transgenic lines, with the exception of *fae1 fad2* plants (**Fig. 6B**). These data suggest that the formation of oleyl-oleate was not limited in wild-type plants by inefficient production of oleyl-alcohol but rather by the specific incorporation of oleate by all variants of *Mm*WS and that the elimination of reactions competing for oleate substrate contributed substantially to the efficient formation of oleyl-alcohol in transgenic *Arabidopsis* plants (Fig. 6).

DISCUSSION

It was the goal of this study to explore the possibility of generating unusual wax esters in transgenic plant seeds and to provide proof of concept in *Arabidopsis*. The aim to produce long chain length monounsaturated wax esters was achieved by using a FAR and a WS from mouse with preference for such substrates, combined with the use of plants displaying enhanced accumulation of oleate as a preferred substrate for the new pathway. Although the selected *Mm*FAR1 and *Mm*WS may have desired specificities, these enzymes do not naturally cooperate in vivo and in fact display dissimilar subcellular localization (5, 6) (Figs. 1 and 2). In this context, the peroxisomal localization of *Mm*FAR1 is of particular interest, as the enzyme does not contain a recognizable PTS. Instead, peroxisomal targeting of *Mm*FAR1 was found to depend on the presence of the C-terminal 66 amino acids (Fig. 1), which represent a putative transmembrane anchor. To our knowledge, *Mm*FAR1 may represent the first example of an enzyme that is targeted to peroxisomes by a C-terminal transmembrane region that is not a component of the peroxisomal protein
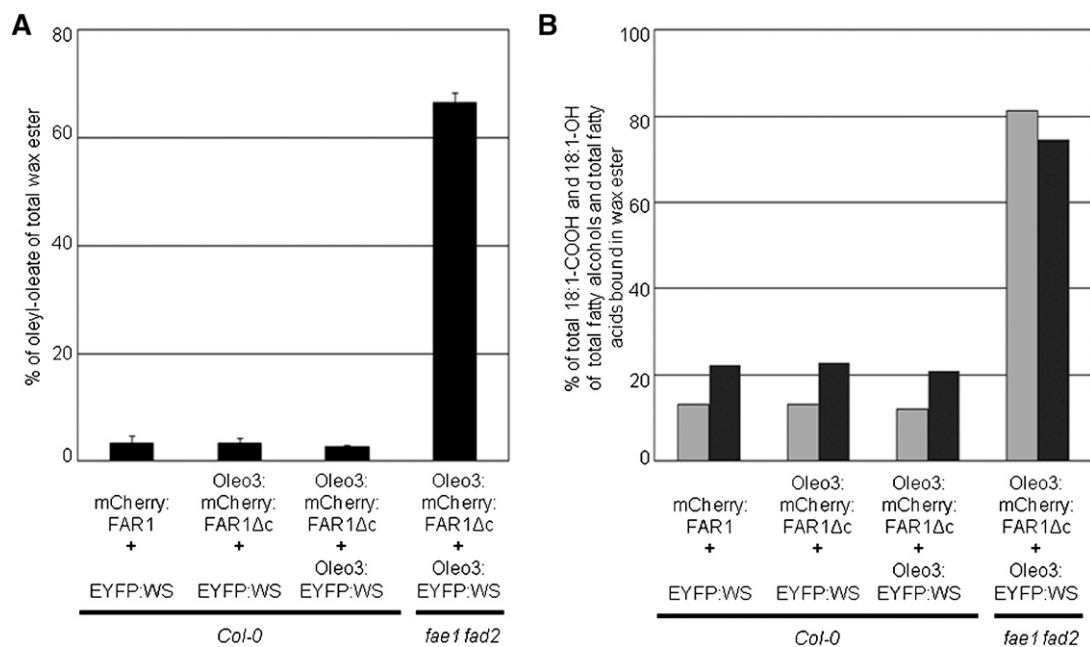

Fig. 5. (A–C) Wax ester profile of *Arabidopsis* Col-0 wt and (D) Col-0 *fae1 fad2* mutant expressing the transgene combinations. (A) mCherry:*Mm*FAR1 + EYFP:*Mm*WS, (B) Oleo3:mCherry:*Mm*FAR1Δc + EYFP:*Mm*WS, and (C, D) Oleo3:mCherry:*Mm*FAR1Δc + Oleo3:EYFP:*Mm*WS. Shown is the mean (+ SD) relative accumulation of the 10 most abundant wax ester species determined by direct infusion nano-ESI-MS^2 analysis of T2 seed stocks from (A) 10, (B) 14, (C) 10, and (D) 6 individual lines.

Fig. 6. Relative incorporation of 18:1-acyl CoA in the total wax ester pool of seeds of *Arabidopsis* Col-0 wt and Col-0 *fae1 fad2* mutant background expressing the indicated transgene combinations. (A) Shown is the mean (+ SD) relative oleyl-oleate accumulation in mol % of total wax ester load of individual heterozygous T2 lines with 10, 14, 10, and 6 lines analyzed. (B) Shown are the relative amounts of wax esters in mol % of total wax esters carrying an 18:1-COOH moiety (gray bar) or an 18:1-OH moiety (black bar). The values represent the sum of means of relative amounts of respective wax ester species.

translocation complex (22). It is furthermore interesting to note that the mechanism of peroxisomal targeting of *Mm*FAR1 is conserved in organisms as diverse as mouse and onion. Based on the dissimilar localization of *Mm*FAR1 and *Mm*WS in mouse and in onion epidermis cells, it is clear that these enzymes normally do not define an efficient pathway to generate wax esters. To achieve a more efficient wax ester production by *Mm*FAR and *Mm*WS, both enzymes were cotargeted by fusing them with *Arabidopsis* oleosin3 (Oleo3). The rationale behind the co-targeting approach was that the joint association in one membrane and even in one membrane microdomain would enable channeling of lipid intermediates, thus preventing alternative reactions that might be detrimental to wax ester production. Indeed, this concept has been identified originally in tung tree seeds that accumulate large amounts of α-eleostearic acid in the seed oil (23). Although we have not shown an association of Oleo3: *Mm*FAR1Δc and Oleo3:*Mm*WS with oil bodies in transgenic *Arabidopsis* seeds, previous data on heterologous expression of oleosins strongly suggest that the oleosin fusion proteins generated in this study localize to oil bodies as well (24). Consequently, this localization to oil bodies may provide a suitable means to sequester hydrophobic reaction products directly into this storage organelle. To achieve cotargeting of *Mm*FAR1 and *Mm*WS to oil bodies, modification of the enzymes was required. As the deletion in *Mm*FAR1 and the fusions of *Mm*FAR1Δc and *Mm*WS to Oleosin3 might have affected folding of the enzymes, the catalytic activity of the modified enzymes in vivo might have been impaired. Control experiments testing the accumulation of fatty alcohols upon expression of nonmodified

and modified variants of *Mm*FAR1 indicate that *Mm*FAR1 was not adversely influenced by the modifications (Fig. 3A). Cotargeting of Oleo3:*Mm*FAR1Δc and Oleo3:*Mm*WS resulted in a greater accumulation of wax esters than was observed upon coexpression of nonmodified enzymes (Fig. 3B). These observations suggest that the efficient co-operativity of Oleo3:*Mm*FAR1Δc and Oleo3:*Mm*WS was a result of close spatial proximity rather than altered catalytic capacity. It is interesting to note that the expression of Oleo3:*Mm*WS in yeast was accompanied by increased levels of triacylglycerol (TAG) in the quadruple yeast mutant (Fig. 3B). Increased TAG levels were not observed upon expression of Oleo3:*Mm*FAR1Δc alone (Fig. 3B). Due to this finding and as the amount of oleosins in seeds regulates oil body size instead of TAG amount (18, 25), the TAG accumulation upon expression of Oleo3:*Mm*WS is likely not only related to an increased abundance of oleosins in the cells. Instead, the increased TAG content observed might be a consequence of the inherent activity of *Mm*WS as a diacylglycerol:acyl-CoA transferase (DAGAT), which results in TAG formation as a side reaction of wax ester formation (6). When the increased levels of wax esters formed upon coexpression of Oleo3:*Mm*FAR1Δc and Oleo3:*Mm*WS in yeast and *Arabidopsis* are compared to those of mCherry:FAR1 and EYFP:MmWS, it becomes obvious that the accumulation of wax esters in yeast is more substantial than that found in *Arabidopsis* (Figs. 3B and 4A). A possible explanation may be that yeast naturally contains mostly oleate, a preferred substrate of *Mm*FAR1 and *Mm*WS, whereas *Arabidopsis* also contains many other fatty acids, even in the *fae1 fad2* mutant, as a consequence of metabolic exchange between the eukaryotic

and prokaryotic pathways of lipid biosynthesis. Clearly, the metabolism of *Arabidopsis* is more complex and will present more side reactions that impair wax ester accumulation. In addition, wax esters formed may interfere with the regulation of storage lipid deposition. Therefore, eliminating the side reactions will provide one possibility to further optimize wax ester accumulation in transgenic plants in the future. By eliminating some of the fatty acid modifications, such as elongation and polyunsaturation in the *Arabidopsis fae1 fad2* mutant, it was possible to obtain wax esters in transgenic plants that contained greater than 65% oleyl-oleate, a molecular wax ester species ranging around only 5% in the wild-type background (Fig. 5). The data presented indicate that efficient formation of unusual wax esters in transgenic plants is feasible and that metabolism can be shaped toward desirable wax ester products, such as oleyl-oleate, by tapping into the wide variety of available fatty acid modification mutants.∎

REFERENCES

1. Biermann, U., U. Bornscheuer, M. A. R. Meier, J. O. Metzger, and H. J. Schäfer. 2011. Oils and fats as renewable raw materials in chemistry. *Angew. Chem. Int. Ed. Engl.* **50:** 3854–3871.
2. Carlsson, A. S., J. L. Yilmaz, A. G. Green, S. Stymne, and P. Hofvander. 2011. Replacing fossil oil with fresh oil – with what and for what? *Eur. J. Lipid Sci. Technol.* **113:** 812–831.
3. Miwa, T. K. 1971. Jojoba oil wax esters and derived fatty acids and alcohols - gas chromatographic analyses. *J. Am. Oil Chem. Soc.* **48:** 259–264.
4. Lardizabal, K. D., J. G. Metz, T. Sakamoto, W. C. Hutton, M. R. Pollard, and M. W. Lassner. 2000. Purification of a Jojoba embryo wax synthase, cloning of its cDNA, and production of high levels of wax in seeds of transgenic Arabidopsis. *Plant Physiol.* **122:** 645–655.
5. Cheng, J. B., and D. W. Russell. 2004. Mammalian wax biosynthesis: I. Identification of two fatty acyl-CoA reductases with different substrate specificities and tissue distributions. *J. Biol. Chem.* **279:** 37789–37797.
6. Cheng, J. B., and D. W. Russell. 2004. Mammalian wax biosynthesis: II. Expression cloning of wax synthase cdnas encoding a member of the acyltransferase enzyme family. *J. Biol. Chem.* **279:** 37798–37807.
7. Maniatis, T., E. F. Fritsch, and J. Sambrook. 1982. Molecular Cloning: A Laboratory Manual. Cold Spring Harbor Laboratory Press, Cold Spring Harbor, NY.
8. Hornung, E., M. Korfei, C. Pernstich, A. Struss, H. Kindl, M. Fulda, and I. Feussner. 2005. Specific formation of arachidonic acid and eicosapentaenoic acid by a front-end Δ⁵-desaturase from Phytophthora megasperma. *Biochim. Biophys. Acta.* **1686:** 181–189.
9. Ellerström, M., K. Stålberg, I. Ezcurra, and L. Rask. 1996. Functional dissection of a napin gene promoter: identification of promoter elements required for embryo and endosperm-specific transcription. *Plant Mol. Biol.* **32:** 1019–1027.
10. De Greve, H., P. Dhaese, J. Seurinck, M. Lemmers, M. Van Montagu, and J. Schell. 1982. Nucleotide sequence and transcript map of the *Agrobacterium tumefaciens* Ti plasmid-encoded octopine synthase gene. *J. Mol. Appl. Genet.* **1:** 499–511.
11. Clough, S. J., and A. F. Bent. 1998. Floral dip: a simplified method for *Agrobacterium*-mediated transformation of *Arabidopsis thaliana.* *Plant J.* **16:** 735–743.
12. Sandager, L., M. H. Gustavsson, U. Stahl, A. Dahlqvist, E. Wiberg, A. Banas, M. Lenman, H. Ronne, and S. Stymne. 2002. Storage lipid synthesis is non-essential in yeast. *J. Biol. Chem.* **277:** 6478–6482.
13. Fulda, M., J. Shockey, M. Werber, F. P. Wolter, and E. Heinz. 2002. Two long-chain acyl-CoA synthetases from *Arabidopsis thaliana* involved in peroxisomal fatty acid β-oxidation. *Plant J.* **32:** 93–103.
14. Ma, C., and S. Reumann. 2008. Improved prediction of peroxisomal PTS1 proteins from genome sequences based on experimental subcellular targeting analyses as exemplified for protein kinases from Arabidopsis. *J. Exp. Bot.* **59:** 3767–3779.
15. Reumann, S., L. Babujee, C. Ma, S. Wienkoop, T. Siemsen, G. E. Antonicelli, N. Rasche, F. Luder, W. Weckwerth, and O. Jahn. 2007. Proteome analysis of *Arabidopsis* leaf peroxisomes reveals novel targeting peptides, metabolic pathways, and defense mechanisms. *Plant Cell.* **19:** 3170–3193.
16. Sonnhammer, E. L., G. von Heijne, and A. Krogh. 1998. A hidden Markov model for predicting transmembrane helices in protein sequences. *Proc. Int. Conf. Intell. Syst. Mol. Biol.* **6:** 175–182.
17. Orth, T., S. Reumann, X. Zhang, J. Fan, D. Wenzel, S. Quan, and J. Hu. 2007. The PEROXIN11 protein family controls peroxisome proliferation in *Arabidopsis. Plant Cell.* **19:** 333–350.
18. Siloto, R. M. P., K. Findlay, A. Lopez-Villalobos, E. C. Yeung, C. L. Nykiforuk, and M. M. Moloney. 2006. The accumulation of oleosins determines the size of seed oilbodies in Arabidopsis. *Plant Cell.* **18:** 1961–1974.
19. Smith, M. A., H. Moon, G. Chowrira, and L. Kunst. 2003. Heterologous expression of a fatty acid hydroxylase gene in developing seeds of *Arabidopsis thaliana. Planta.* **217:** 507–516.
20. Kunst, L., D. C. Taylor, and E. W. Underhill. 1992. Fatty acid elongation in developing seeds of *Arabidopsis thaliana. Plant Physiol. Biochem.* **30:** 425–434.
21. Okuley, J., J. Lightner, K. Feldmann, N. Yadav, E. Lark, and J. Browse. 1994. Arabidopsis FAD2 gene encodes the enzyme that is essential for polyunsaturated lipid synthesis. *Plant Cell.* **6:** 147–158.
22. Ma, C., G. Agrawal, and S. Subramani. 2011. Peroxisome assembly: matrix and membrane protein biogenesis. *J. Cell Biol.* **193:** 7–16.
23. Shockey, J. M., S. K. Gidda, D. C. Chapital, J-C. Kuan, P. K. Dhanoa, J. M. Bland, S. J. Rothstein, R. T. Mullen, and J. M. Dyer. 2006. Tung tree DGAT1 and DGAT2 have nonredundant functions in triacylglycerol biosynthesis and are localized to different subdomains of the endoplasmic reticulum. *Plant Cell.* **18:** 2294–2313.
24. Boothe, J., C. Nykiforuk, Y. Shen, S. Zaplachinski, S. Szarka, P. Kuhlman, E. Murray, D. Morck, and M. M. Moloney. 2010. Seed-based expression systems for plant molecular farming. *Plant Biotechnol. J.* **8:** 588–606.
25. Vieler, A., S. B. Brubaker, B. Vick, and C. Benning. 2012. A lipid droplet protein of Nannochloropsis with functions partially analogous to plant oleosins. *Plant Physiol.* **158:** 1562–1569.